OXFORD

Human Molecular Genetics, 2017, *Vol. 26, No. 10* 1915–1926

doi: 10.1093/hmg/ddx100
Advance Access Publication Date: 24 March 2017
Original Article

ORIGINAL ARTICLE

Sirt3 protects dopaminergic neurons from mitochondrial oxidative stress

Han Shi[1], Han-Xiang Deng[2], David Gius[3], Paul T. Schumacker[4], D. James Surmeier[5] and Yong-Chao Ma[1,*]

[1]Departments of Pediatrics, Neurology and Physiology, Northwestern University Feinberg School of Medicine, Anne & Robert H. Lurie Children's Hospital of Chicago, Chicago, IL, USA, [2]The Ken & Ruth Davee Department of Neurology, [3]Department of Radiology, Lurie Cancer Institute, [4]Department of Pediatrics and [5]Department of Physiology, Northwestern University Feinberg School of Medicine, Chicago, IL 60611, USA

*To whom correspondence should be addressed. Tel: 7737556393; Fax: 7737556385; Email: ma@northwestern.edu

Abstract

Age-dependent elevation in mitochondrial oxidative stress is widely posited to be a major factor underlying the loss of substantia nigra pars compacta (SNc) dopaminergic neurons in Parkinson's disease (PD). However, mechanistic links between aging and oxidative stress are not well understood. Sirtuin-3 (Sirt3) is a mitochondrial deacetylase that could mediate this connection. Indeed, genetic deletion of *Sirt3* increased oxidative stress and decreased the membrane potential of mitochondria in SNc dopaminergic neurons. This change was attributable to increased acetylation and decreased activity of manganese superoxide dismutase (MnSOD). Site directed mutagenesis of lysine 68 to glutamine (K68Q), mimicking acetylation, decreased MnSOD activity in SNc dopaminergic neurons, whereas mutagenesis of lysine 68 to arginine (K68R), mimicking deacetylation, increased activity. Introduction of K68R MnSOD rescued mitochondrial redox status and membrane potential of SNc dopaminergic neurons from *Sirt3* knockouts. Moreover, deletion of *DJ-1*, which helps orchestrate nuclear oxidant defenses and *Sirt3* in mice led to a clear age-related loss of SNc dopaminergic neurons. Lastly, K68 acetylation of MnSOD was significantly increased in the SNc of PD patients. Taken together, our studies suggest that an age-related decline in Sirt3 protective function is a major factor underlying increasing mitochondrial oxidative stress and loss of SNc dopaminergic neurons in PD.

Introduction

Parkinson's disease (PD) is the second most common neurodegenerative disorder (1,2). The cardinal motor symptoms of PD—bradykinesia and rigidity—are due to the selective degeneration of dopaminergic neurons in the substantia nigra pars compacta (SNc) (3,4). There are several potential causes of SNc degeneration in PD but age is the largest risk factor, with one in every 50 people over the age of 60 years being afflicted (1,2,5,6). Why age is the principal risk factor for the loss of SNc dopaminergic neurons is uncertain.

What is known is that mitochondrial dysfunction is central to the etiology of PD and the selective loss of SNc dopaminergic neurons. Mitochondrial oxidative phosphorylation (OXPHOS) is widely viewed as being necessary to meet the bioenergetic needs of neurons (7,8). In the SNc of PD patients, there are deficits in electron transport chain (ETC) Complex I function and abnormal accumulation of mitochondrial DNA mutations (9–11). Both deficits will compromise the ability of mitochondria to meet neuronal bioenergetic demands. One potential cause of these deficits is mitochondrial oxidative stress. In both rodent

Received: January 13, 2017. **Revised:** March 7, 2017. **Accepted:** March 9, 2017

and human SNc dopaminergic neurons, basal mitochondrial oxidative stress is elevated (12–14). This elevation is attributable to autonomous pacemaking activity in these neurons that leads to sustained, Ca^{2+}-mediated stimulation of OXPHOS (15,16). Reactive oxygen species (ROS) are an unavoidable byproduct of OXPHOS. ROS damage proteins, DNA and lipids, making them obvious culprits in the mitochondrial damage seen in PD patients. The centrality of mitochondrial oxidative stress in the etiology of PD is supported by the recognition that early onset forms of familial PD are caused by loss of function mutations in genes regulating mitochondrial oxidant defenses (*DJ-1*) or mitochondrial quality control (*PINK1*, *parkin/PARK2*) (16–20).

But how is aging connected to this phenomenon? An age-dependent decline in the protective function of sirtuins is one possibility. Sirtuins are a family of metabolically regulated deacetylases (21,22). One of the sirtuins—Sirtuin-3 (Sirt3)—is preferentially localized to mitochondria. By deacetylating mitochondrial proteins, Sirt3 plays a critical role in regulating OXPHOS and mitochondrial oxidative stress (23–27). One recently discovered target of Sirt3 is manganese superoxide dismutase (MnSOD). MnSOD is the primary mitochondrial enzyme converting superoxide generated by OXPHOS to hydrogen peroxide, which is converted to water by catalase (28). Thus, declining Sirt3 function with age could lead to declining MnSOD activity in SNc dopaminergic neurons and elevated mitochondrial oxidative stress. Ultimately, this oxidative stress could overwhelm mitochondrial defenses and quality control mechanisms, triggering cell death.

This study was aimed at testing this hypothesis. To this end, SNc dopaminergic neurons in *Sirt3* knockout mice were studied using a combination of approaches. In mice, the loss of Sirt3 led to increased acetylation of MnSOD on lysine 68 and decreased MnSOD dismutase activity, resulting in increased mitochondrial oxidant and loss of mitochondrial membrane potential. A similar elevation in acetylation of MnSODK68 was found in the SNc of PD patients. Moreover, in mice lacking functional *DJ-1*, *Sirt3* deletion increased oxidative stress in SNc dopaminergic neurons and led to their progressive loss *in vivo*, mimicking the age-dependent loss in PD. Thus, the age-dependent decline of Sirt3 function in SNc dopaminergic neurons could be a major factor in PD pathogenesis, opening new therapeutic avenues for disease-modifying, neuroprotective strategies.

Results

Sirt3 deacetylates MnSOD on lysine 68 in SNc dopaminergic neurons

As a first step toward elucidating the mechanisms by which Sirt3 might protect SNc dopaminergic neurons, its role in deacetylating MnSOD was determined. Previous studies have suggested that lysine 68 (K68) on MnSOD is a potential deacetylation target for Sirt3 (29–31). Sequence alignment showed that lysine 68 is highly conserved across species (Fig. 1A). In mitochondria, functional MnSOD is a homotetramer (32). Lysine 68 is located at the end of helix 1α of each subunit. This position is close to the type I tight turn connecting helix 1α1 and 2α, which forms a helical hairpin that is critical for the access of ROS to the active site of MnSOD (Fig. 1B) (33,34). To study the Sirt3-mediated deacetylation of lysine 68, an antibody was developed that recognized MnSOD only when it is acetylated on lysine 68 (the acetyl-MnSOD K68 antibody). The affinity purified acetyl-MnSOD K68 antibody specifically recognized wild type (WT) form of MnSOD that was acetylated on lysine 68 in MN9D cells, a dopaminergic neuron derived cell line (35); the antibody did not bind to a mutant form of MnSOD where the lysine 68 residue had been mutated to arginine (K68R) and could not be acetylated (Fig. 1C). The acetyl-MnSOD K68 antibody also recognized the K122R mutant form of MnSOD, which served as a control. Introduction of the mutant forms of MnSOD did not affect the overall expression level of the protein (Fig. 1C).

To test whether Sirt3 mediates the deacetylation of MnSOD in dopaminergic neurons *in vivo*, the acetyl-MnSOD K68 antibody was used to examine brain tissue. Mouse ventral midbrain tissue containing SNc dopaminergic neurons was micro-dissected and tested for MnSOD K68 acetylation. Western blot analysis showed significantly higher acetylation of MnSOD K68 in *Sirt3* knockout mice than that in WT mice (Fig. 1D), while the expression levels of MnSOD protein in *Sirt3* knockout mice and WT mice were similar. These results provide compelling evidence that Sirt3 deacetylates MnSOD on lysine 68 in mouse SNc dopaminergic neurons.

Acetylation of lysine 68 decreases MnSOD activity in SNc dopaminergic neurons

Next, the role of lysine 68 acetylation in regulating the superoxide dismutase activity of MnSOD in SNc dopaminergic neurons was determined. Superoxide dismutase activity was measured using a tetrazolium-based colorimetric assay (Cayman Chemical). SNc tissue from WT and *Sirt3*$^{-/-}$ mice at 5 months and 15 months of age was micro-dissected and mitochondria isolated to allow mitochondrial MnSOD activity to be distinguished from that of cytosolic Cu/ZnSOD and FeSOD. In 5-month-old *Sirt3*$^{-/-}$ mice, mitochondrial MnSOD activity, but not cytosolic SOD activity, was decreased (Fig. 2A). Similarly, in 15-month-old *Sirt3*$^{-/-}$ mice, mitochondrial MnSOD activity, but not cytosolic SOD activity, was decreased (Fig. 2B).

To determine if Sirt3 regulated MnSOD activity in situ, MN9D cells were used. In these cells, WT MnSOD, the deacetylation-mimetic K68R mutant form of MnSOD and the acetylation-mimetic K68Q mutant form of MnSOD were expressed and then MnSOD activity was measured using the Cayman Chemical colorimetric assay. MN9D cells expressing WT MnSOD had higher mitochondrial MnSOD activity relative to untransfected cells. Expression of the deacetylation-mimetic MnSOD K68R led to an even greater increase of the dismutase activity in mitochondria (Fig. 2C). In contrast, expression of MnSOD K68Q, which mimics the acetylated form of MnSOD, did not lead to any significant change of SOD activity compared with untransfected cells (Fig. 2C). Cytosolic SOD activities in MN9D cells expressing WT, K68R or K68Q forms of MnSOD were at the same level as non-transfected cells (data not shown). These results suggest that Sirt3-mediated deacetylation of MnSOD on lysine 68 increases MnSOD activity in dopaminergic neurons.

Sirt3 deacetylation of MnSOD K68 decreases mitochondrial oxidative stress

MnSOD mitigates mitochondrial oxidative stress. Hence, decreasing its activity should increase mitochondrial oxidative stress in SNc dopaminergic neurons. To test this hypothesis, a redox-sensitive variant of green fluorescent protein (roGFP) with a mitochondrial-matrix-targeting sequence (mito-roGFP) under the control of tyrosine hydroxylase (TH) promoter was expressed in SNc dopaminergic neurons *in vitro* (16). Mitochondrial oxidative stress was then measured by live cell fluorescence imaging (Fig. 3A and B). As predicted, oxidative stress in SNc dopaminergic neurons from *Sirt3* knockouts was significantly greater than that in SNc dopaminergic neurons

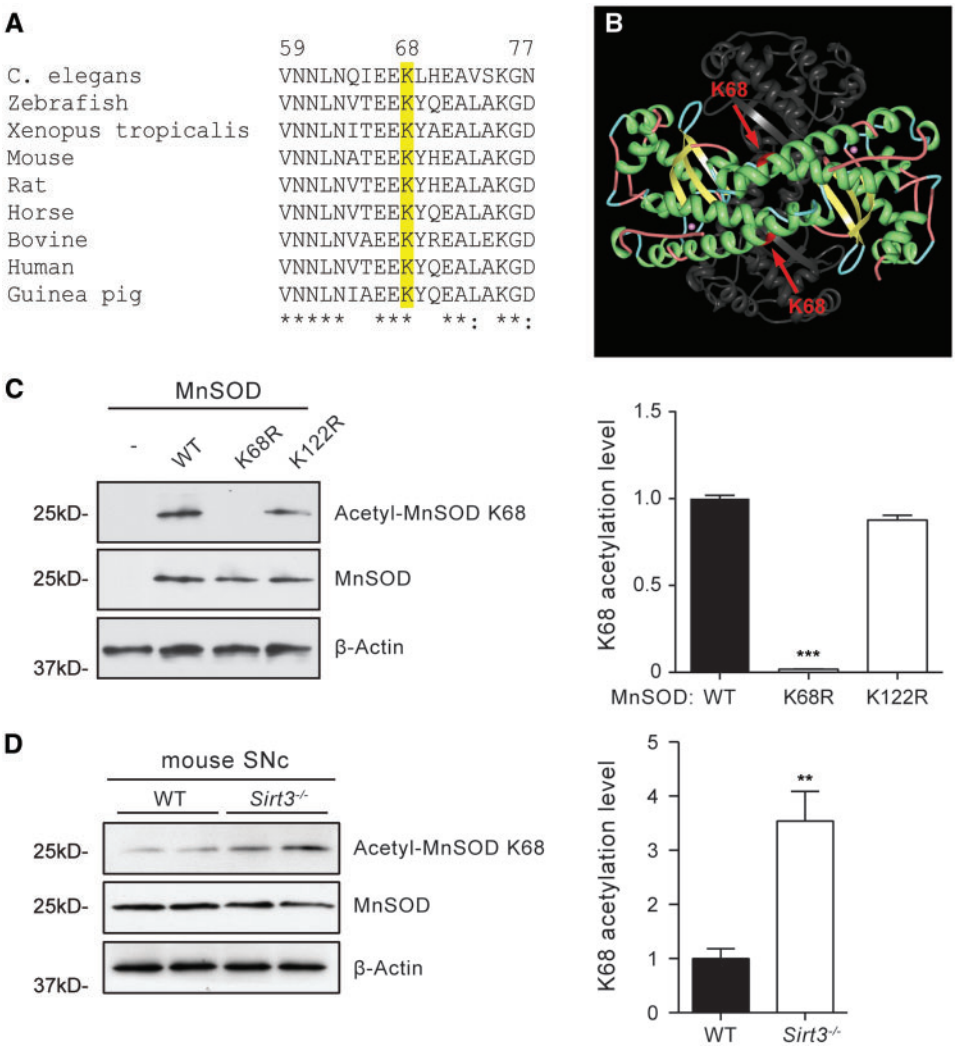

Figure 1. Sirt3 deacetylates MnSOD on Lysine 68 in SNc dopaminergic neurons. **(A)** Amino acid sequence alignment showing that lysine 68 (K68) is conserved across species. **(B)** Position of lysine 68 within the three dimensional structure of MnSOD. The structure of four identical MnSOD subunits is shown in ribbon diagram, with two subunits presented in colors and two in light grey. Lysine 68 is displayed in red and pointed by arrow. Two manganese ions that are essential for MnSOD structure and function are shown in magenta. **(C)** Western blot analysis of MnSOD acetylation on lysine 68 using the acetyl-MnSOD K68 specific antibody. Mouse dopaminergic neurons transfected with WT MnSOD and K122R mutant form of MnSOD showed high levels of acetylation of MnSOD K68, but there was no acetylation on K68 in cells transfected with the MnSOD K68R mutant, demonstrating the specificity of the antibody. Data were quantified by densitometry from four independent experiments and are mean ± SEM. ***$P < 0.001$, one-way ANOVA with Tukey's HSD *post hoc* analysis. **(D)** Western blot analysis of MnSOD acetylation on lysine 68 in *Sirt3*$^{-/-}$ mouse SNc brain tissues. Acetylation of MnSOD on K68 recognized by the acetyl-MnSOD K68 specific antibody was significantly increased in *Sirt3*$^{-/-}$ mice. **$P < 0.01$, Student's *t* test.

from WT mice (Fig. 3C). To determine whether the increase of oxidative stress was caused by Sirt3 deficiency, a Sirt3 expression construct was transfected into neurons. Sirt3 expression rescued mitochondrial oxidative stress in *Sirt3* knockout dopaminergic neurons (Fig. 3C).

To determine whether Sirt3 also plays a similar role in reducing genetically induced mitochondrial oxidative stress, SNc dopaminergic neurons in *Sirt3*$^{-/-}$; *DJ-1*$^{-/-}$ double knockout mice were examined. Loss of function mutations in *DJ-1* (also known as *PARK7* in humans and *Park7* in mice) are associated with autosomal recessive early onset PD (17,18). As previously shown in (16), *DJ-1*$^{-/-}$ SNc dopaminergic neurons had significantly elevated mitochondrial oxidative stress compared with WT SNc dopaminergic neurons (Fig. 3D). Deletion of *Sirt3* further increased oxidative stress in *DJ-1*$^{-/-}$ SNc dopaminergic neurons (Fig. 3D). Moreover, transfection of *Sirt3* into the double knockout neurons diminished mitochondrial oxidative stress (Fig. 3D).

To test the hypothesis that the Sirt3 effect was mediated by deacetylation of MnSOD, the deacetylation-mimetic MnSOD K68R was expressed in *Sirt3*$^{-/-}$ and *Sirt3*$^{-/-}$; *DJ-1*$^{-/-}$ SNc dopaminergic neurons. In both cases, MnSOD68 expression effectively compensated for *Sirt3* deletion (Fig. 3C and D). These data are consistent with the hypothesis that Sirt3-mediated deacetylation of MnSOD K68 diminishes mitochondrial oxidative stress in SNc dopaminergic neurons.

Deacetylation of MnSOD on lysine 68 restores mitochondrial membrane potential

One of the principal consequences of mitochondrial oxidative stress is thought to be damage to proteins of the ETC. The ETC

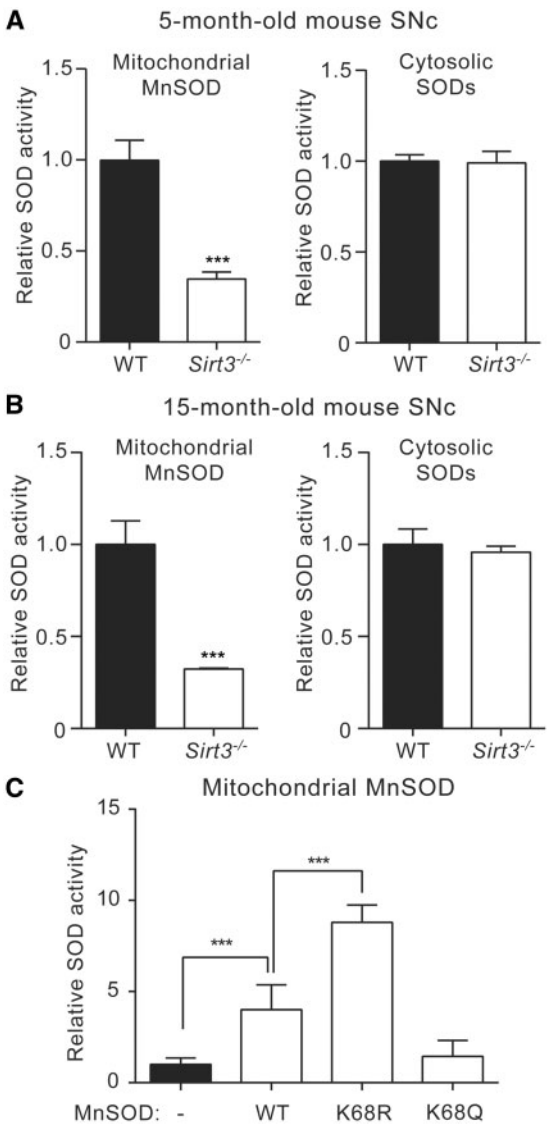

Figure 2. Acetylation of lysine 68 decreases MnSOD activity in dopaminergic neurons. **(A)** Activities of mitochondrial MnSOD and cytosolic SODs in 5-month-old WT and *Sirt3*$^{-/-}$ mouse SNc. Mitochondrial MnSOD activity in *Sirt3*$^{-/-}$ mouse SNc (n = 9) was significantly reduced than that from WT mice (n = 9), whereas no difference was detected for cytosolic SOD activities (n = 9 for WT, n = 9 for *Sirt3*$^{-/-}$ mice). **(B)** Activities of mitochondrial MnSOD and cytosolic SODs in 15-month-old WT or *Sirt3*$^{-/-}$ mouse SNc. MnSOD from *Sirt3*$^{-/-}$ mice (n = 9) showed significantly lower activity compared with that from WT mice (n = 9), with no difference detected for cytosolic SODs (n = 9 for WT, n = 9 for *Sirt3*$^{-/-}$ mice). **(C)** Mitochondrial MnSOD activity in MN9D cells transfected with WT, K68R or K68Q forms of MnSOD. MnSOD activity was significantly increased in cells expressing MnSOD K68R compared with those expressing WT MnSOD. Cells expressing MnSOD K68Q showed comparable mitochondrial SOD activity as non-transfected cells (n = 9). Data are mean ± SEM. ***$P < 0.001$, Student's *t* test or one-way ANOVA with Tukey's HSD *post hoc* analysis.

serves to pump protons from the matrix and establish a steep electrochemical gradient across the inner mitochondrial membrane (IMM) that is used by Complex V to convert adenosine diphosphate into adenosine triphosphate (ATP). Thus, damage to the ETC manifests itself as a loss of potential. To determine if *Sirt3* deletion could lead to ETC damage and loss of IMM potential, the cationic dye tetramethylrhodamine ethyl (TMRE) was used to examine SNc dopaminergic neurons. Neurons were also infected with adeno-associated virus (AAV)-TH-GFP to allow unequivocal identification of dopaminergic neurons. Indeed, the TMRE fluorescence of dopaminergic neurons from *Sirt3*$^{-/-}$ mice and *DJ-1*$^{-/-}$ mice was significantly less than that of dopaminergic neurons from WT mice (Fig. 4C and D). *Sirt3*$^{-/-}$/*DJ-1*$^{-/-}$ had even more compromised IMM potentials as estimated with TMRE (Fig. 4C and D). Importantly, the expression of a mouse Sirt3 transcript or the deacetylation-mimetic MnSOD K68R compensated for the loss of Sirt3 on IMM potential in dopaminergic neurons from either *Sirt3*$^{-/-}$ or *Sirt3*$^{-/-}$/*DJ-1*$^{-/-}$ dopaminergic neurons (Fig. 4C and D). These results suggest that the elevation in oxidative stress created by the loss of *Sirt3* and diminished MnSOD activity is sufficient to produce damage to the ETC, compromising the ability of mitochondria to produce ATP.

Genetic deletion of *Sirt3* increases the degeneration of SNc dopaminergic neurons

A sustained elevation in mitochondrial oxidative stress—like that seen in *DJ-1*$^{-/-}$, *Sirt3*$^{-/-}$ and *Sirt3*$^{-/-}$/*DJ-1*$^{-/-}$ SNc dopaminergic neurons—is widely hypothesized to result in their death and the emergence of motor symptoms in PD (12–15,36). As a first step toward testing this hypothesis, SNc dopaminergic neurons were examined in cell culture. Cell death was measured by the TUNEL (terminal deoxynucleotidyl transferase dUTP nick end labeling) assay (Fig. 4E and F). Neurons from *Sirt3*$^{-/-}$ and *DJ-1*$^{-/-}$ mice died more than neurons from WT mice (Fig. 4E and F). *Sirt3*$^{-/-}$; *DJ-1*$^{-/-}$ neurons died at a higher rate than neurons lacking only *Sirt3* or *DJ-1* alone (Fig. 4E and F). Moreover, expression of Sirt3 or the deacetylation-mimetic MnSOD K68R slowed cell death in cultures from *Sirt3*$^{-/-}$ and *Sirt3*$^{-/-}$/*DJ-1*$^{-/-}$ mice (Fig. 4E and F).

However, the stressors driving SNc dopaminergic neuron loss in culture are not likely to be identical to those found *in vivo*. So, the degeneration of SNc dopaminergic neurons was examined in mice by immunohistochemical staining and stereological counting of TH-positive SNc dopaminergic neurons. Indeed, as previously reported, deletion of *Sirt3* or *DJ-1* alone did not result in a significant loss of TH staining of SNc dopaminergic neurons at 2 weeks, 5 or 15 months of age (Fig. 5). In 2-week-old *Sirt3*$^{-/-}$; *DJ-1*$^{-/-}$ SNc, there was no change in the abundance of dopaminergic neurons (data not shown), suggesting that this combination did not have deleterious developmental effects. However, by 5 months of age, there was a significant loss of SNc dopaminergic neurons in *Sirt3*$^{-/-}$; *DJ-1*$^{-/-}$ mice (Fig. 5A and B). To verify that this was not simply phenotypic down-regulation of TH, neurons were quantified using a Nissl stain and stereological techniques (Fig. 5C). These counts confirmed the loss of SNc dopaminergic neurons. Moreover, by 15 months of age, the loss of SNc dopaminergic neurons in *Sirt3*$^{-/-}$; *DJ-1*$^{-/-}$ double knockout mice was more pronounced (Fig. 5B and E). Together, these data suggest that Sirt3 protects mouse SNc dopaminergic neurons from age-dependent elevation of mitochondrial oxidative stress and degeneration.

Increased acetylation of MnSOD K68 in PD patients

If Sirt3-mediated deacetylation of MnSOD K68 plays a role in the evolution of PD, MnSOD K68 acetylation should be elevated in the brains of PD patients. To test this hypothesis, SNc tissue from PD patients and age-matched controls was probed with the acetyl-MnSOD K68 antibody in Western blots. Remarkably, there was significantly greater K68 acetylation of MnSOD in the PD samples than in those from controls (Fig. 6A and B). These

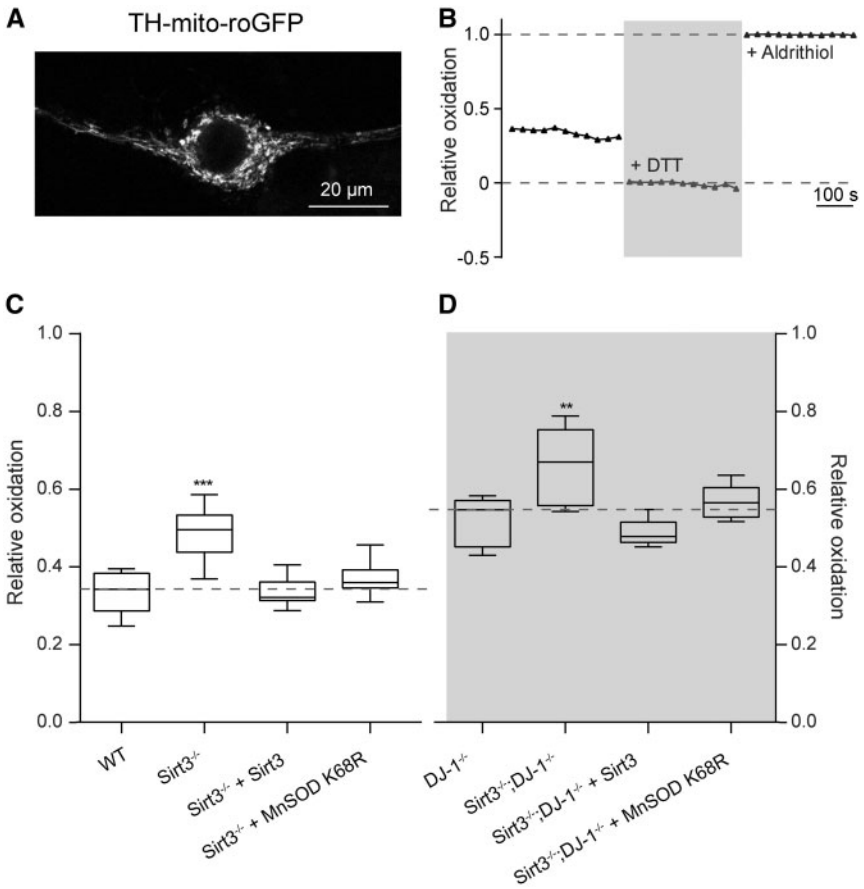

Figure 3. Sirt3-mediated deacetylation of MnSOD K68R decreases mitochondrial oxidative stress. **(A)** Representative image showing the expression of a redox-senstive roGFP with a mitochondria matrix-targeting sequence under the control of TH promoter (TH-mito-roGFP) in dopaminergic neurons. **(B)** Measurement of TH-mito-roGFP relative oxidation level, an assessment of mitochondrial oxidative stress, by quantifying the intensities of TH-mito-roGFP in dopaminergic neurons using a fluorescence live imaging system. DTT and aldrithiol were applied to neurons sequentially to fully reduce (+DTT) or fully oxidize (+Aldrithiol) roGFP for determining its relative oxidation levels. The intensity of roGFP was measured every 30 s. **(C)** Mitochondrial oxidative stress levels measured by TH-mito-roGFP was significantly increased in dopaminergic neurons from *Sirt3*$^{-/-}$ mice than that from WT mice (n = 8). Expression of Sirt3 (n = 8) or MnSOD K68R (n = 8) reduced mitochondrial oxidative stress in *Sirt3*$^{-/-}$ mouse dopaminergic neurons back to the WT level. In these box plots, the median was plotted as the central bar of the box, the upper and lower quartiles were the edges of the box, and the whiskers showed the extremes of the distribution. **(D)** Mitochondrial oxidative stress was significantly increased in neurons from *DJ-1*$^{-/-}$ mice compared with WT mice in (C) (n = 8, $P < 0.0001$, Student's *t* test). Although *Sirt3*$^{-/-}$; *DJ-1*$^{-/-}$ double knockout mice showed even higher level of oxidative stress than *DJ-1*$^{-/-}$ mice (n = 8). Expression of Sirt3 (n = 8) or MnSOD K68R (n = 8) in *Sirt3*$^{-/-}$; *DJ-1*$^{-/-}$ double knockout mouse dopaminergic neurons reduced oxidative stress to the level in *DJ-1*$^{-/-}$ mice. Data are mean ± SEM. ***$P < 0.001$, **$P < 0.01$, one-way ANOVA with Tukey's HSD *post hoc* analysis.

data are clearly consistent with the hypothesis that loss of Sirt3 function, increased acetylation of MnSOD and increased mitochondrial oxidative stress contributes to pathogenesis in PD.

Discussion

Age-dependent elevation in mitochondrial oxidative stress contributes to the selective degeneration of SNc dopaminergic neurons in both familial and idiopathic forms of PD (12–15,36). However, it is unclear how aging leads to mitochondrial oxidative stress. Here we identified Sirt3 as a mediator of this connection by protecting dopaminergic neurons from mitochondrial oxidative stress. In *Sirt3* knockout mice, we found increased acetylation of MnSOD on lysine 68 and decreased MnSOD activity, leading to increased mitochondrial oxidant, reduced mitochondria membrane potential and increased dopaminergic neuron degeneration. These defects could be rescued by expressing Sirt3 or the deacetylation-mimetic MnSOD K68R. Intriguingly, a similar elevation in acetylation of MnSODK68 was found in PD patient SNc tissues, suggesting a critical role for age-dependent decline of Sirt3 protection of mitochondrial oxidative stress in dopaminergic neuron degeneration and PD pathogenesis.

Sirt3 protects aging dopaminergic neurons from endogenous mitochondrial oxidative stress

Using *Sirt3* knockout mice, we found for the first time that Sirt3 protects SNc dopaminergic neurons from oxidative stress generated in their own mitochondria. SNc dopaminergic neurons are characterized by calcium-mediated autonomous pacemaking activity, which comes at a metabolic cost and generates extra oxidative stress as a byproduct of OXPHOS (15,16,36). The age-dependent accumulation of mitochondrial oxidative stress evoked by pacemaking activity, together with oxidative stress generated by dopamine oxidation, contributes to the selective degeneration of SNc dopaminergic neurons in the familiar and idiopathic forms of PD (6,15,37–39). These findings prompted us to focus on the function of Sirt3 specifically in dopaminergic neurons related to PD. Here we identified a role for Sirt3 in

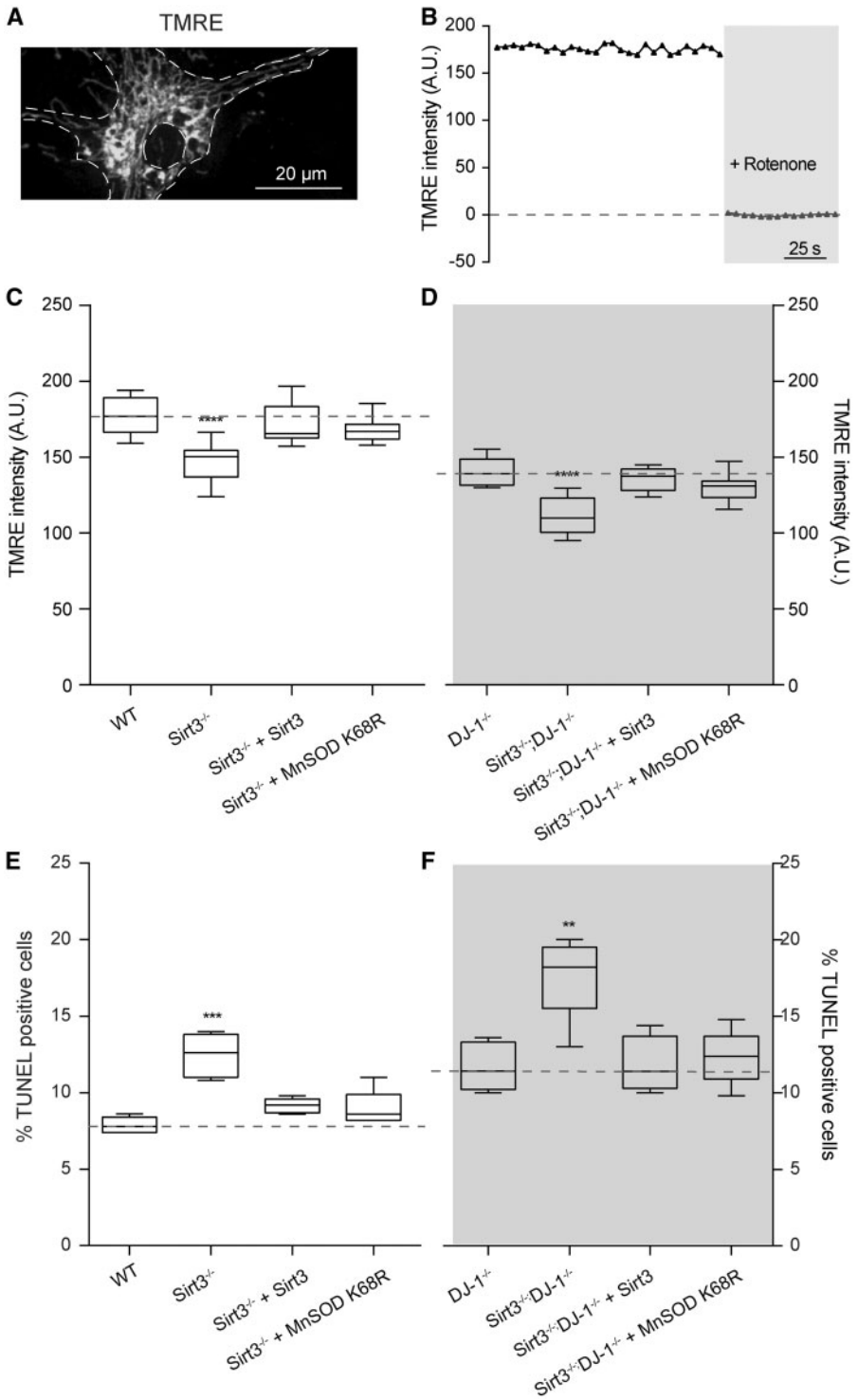

Figure 4. Deacetylation of MnSOD on lysine 68 restores mitochondrial membrane potential and reduces dopaminergic neuron degeneration. **(A)** Representative image showing a dopaminergic neuron stained with TMRE to measure mitochondrial membrane potential. **(B)** Measurement of mitochondrial membrane potential. The intensity of TMRE fluorescent signal in each TH-GFP positive dopaminergic neurons was measured every 5 s using a live imaging system. Rotenone was applied to completely disrupt mitochondrial membrane potential and determine the baseline of TMRE fluorescent signal. **(C)** Mitochondrial membrane potential in dopaminergic neurons from *Sirt3*$^{-/-}$ mice (n = 8) was significantly lower than that in WT mice (n = 8). Expression of Sirt3 (n = 8) or MnSOD K68R (n = 8) restored the membrane potential in *Sirt3*$^{-/-}$ mice back to the WT level. **(D)** Mitochondrial membrane potential in dopaminergic neurons from *DJ-1*$^{-/-}$ knockout mice was significantly reduced than that in WT mice in (C) (n = 8, $P < 0.01$, Student's *t* test). Although *Sirt3*$^{-/-}$; *DJ-1*$^{-/-}$ double knockout mouse dopaminergic neurons (n = 8) showed even lower mitochondrial membrane potential than those from *DJ-1*$^{-/-}$ mice (n = 8). Expression of Sirt3 (n = 8) or MnSOD K68R (n = 8) in *Sirt3*$^{-/-}$; *DJ-1*$^{-/-}$ double knockout neurons restored mitochondrial membrane potential back to the level in *DJ-1*$^{-/-}$ mouse neurons. **(E)** Quantification of TUNEL-positive degenerating dopaminergic neurons from WT and *Sirt3*$^{-/-}$ mice. Ventral midbrain neurons from *Sirt3*$^{-/-}$ mice (n = 8) showed significantly higher percentage of TUNEL-positive cells than those from WT mice (n = 8). Expression of Sirt3 (n = 8) or MnSOD K68R (n = 8) reduced degeneration in *Sirt3*$^{-/-}$ dopaminergic neurons back to the WT level. **(F)** The percentage of TUNEL-positive degenerating dopaminergic neurons from *DJ-1*$^{-/-}$ knockout mice was significantly higher than that in WT mice in (E) (n = 8, $P < 0.01$, Student's *t* test). Although *Sirt3*$^{-/-}$; *DJ-1*$^{-/-}$ double knockout mice (n = 8) showed even more degenerating dopaminergic neurons than those from *DJ-1*$^{-/-}$ mice (n = 8). Expression of Sirt3 or MnSOD K68R in neurons from *Sirt3*$^{-/-}$; *DJ-1*$^{-/-}$ double knockout mice reduced degeneration to the level in *DJ-1*$^{-/-}$ mice (n = 8). Data are mean ± SEM. ****$P < 0.0001$, ***$P < 0.001$, **$P < 0.01$, one-way ANOVA with Tukey's HSD *post hoc* analysis.

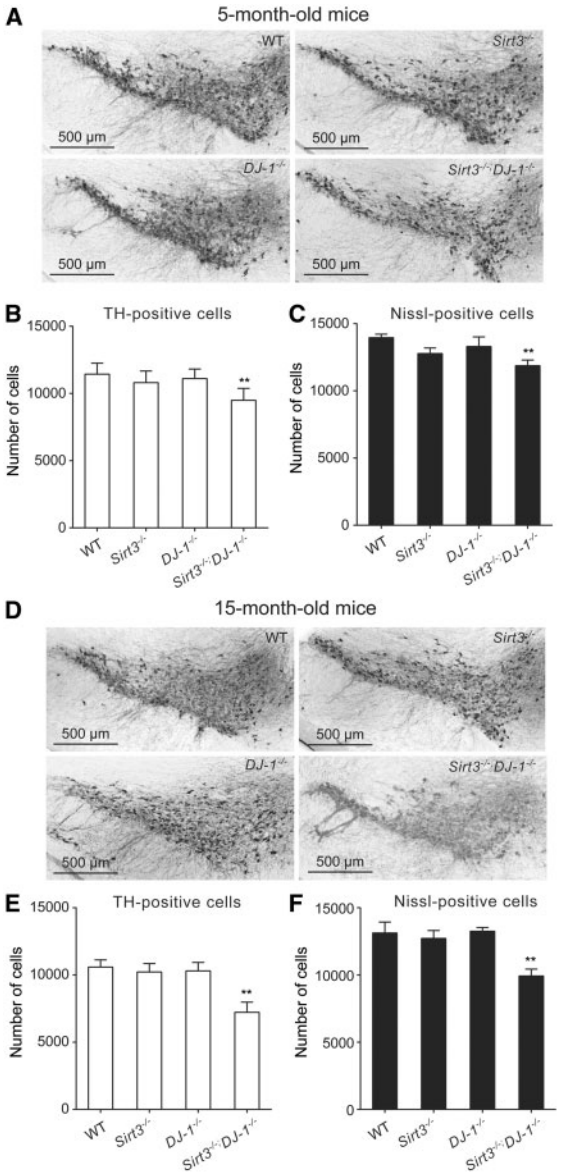

Figure 5. Genetic knockout of *Sirt3* increases SNc dopaminergic neuron degeneration induced by mitochondrial oxidative stress in mice. **(A)** Immunohistochemical staining of TH-expressing dopaminergic neuron in ventral midbrain of 5-month-old WT, *DJ-1*$^{-/-}$, *Sirt3*$^{-/-}$ and *Sirt3*$^{-/-}$; *DJ-1*$^{-/-}$ mice. **(B,C)** Bar graph summarizing numbers of dopaminergic neurons quantified by TH staining and total numbers of neurons by Nissl staining in 5-month-old mice. Number of SNc dopaminergic neurons in *Sirt3*$^{-/-}$; *DJ-1*$^{-/-}$ double knockout mice (n = 6) was significantly ($P < 0.002$) reduced compared with the number in WT mice (n = 8), whereas there was no significant change in *DJ-1*$^{-/-}$ mice (n = 8) or *Sirt3*$^{-/-}$ mice (n = 6). Total number of neurons in *Sirt3*$^{-/-}$; *DJ-1*$^{-/-}$ double knockout mice (n = 6) quantified by Nissl staining was also significantly reduced ($P < 0.002$) compared with WT (n = 8), *DJ-1*$^{-/-}$ (n = 8), and *Sirt3*$^{-/-}$ mice (n = 6). **(D)** Immunostaining of TH-positive dopaminergic neurons in the ventral midbrain of 15-month-old WT, *DJ-1*$^{-/-}$, *Sirt3*$^{-/-}$ and *Sirt3*$^{-/-}$; *DJ-1*$^{-/-}$ mice. **(E,F)** Bar graph summarizing the number of dopaminergic neurons and the total number of neurons in the substantia nigra of 15-month-old mice. *Sirt3*$^{-/-}$; *DJ-1*$^{-/-}$ double knockout mice (n = 6) showed significantly ($P < 0.002$) decreased number of SNc dopaminergic neurons, compared with WT (n = 8), *DJ-1*$^{-/-}$ mice (n = 8) and *Sirt3*$^{-/-}$ mice (n = 6). By 15 months of age, the degeneration of SNc dopaminergic neurons in these double knockout mice were more pronounced than that in 5-month-old double knockouts ($P < 0.002$). Total number of neurons in *Sirt3*$^{-/-}$; *DJ-1*$^{-/-}$ double knockout mice (n = 6) quantified by Nissl staining was also significantly reduced ($P < 0.002$) compared with WT (n = 8), *DJ-1*$^{-/-}$ (n = 8), and *Sirt3*$^{-/-}$ mice (n = 6). Data are mean ± SEM. **$P < 0.01$, one-way ANOVA with Tukey's HSD *post hoc* analysis.

protecting dopaminergic neurons from endogenous mitochondrial oxidative stress. This role is more relevant to PD pathogenesis than the function of Sirt3 in MPTP (1-methyl-4-phenyl-1,2,3,6-tetrahydropyridine) toxicity (40,41), because MPTP-induced dopaminergic neuron death does not occur in PD (42–44). Elucidating mechanisms by which Sirt3 protects SNc dopaminergic neurons from intrinsic mitochondrial oxidative stress has strong implications not only for understanding the pathogenesis of PD but also for developing therapies.

In addition to increased mitochondrial oxidative stress (Fig. 3) and reduced mitochondrial membrane potential (Fig. 4A–D), *Sirt3*$^{-/-}$; *DJ-1*$^{-/-}$ double knockout mice also showed the Parkinsonian phenotype of selective dopaminergic neuron degeneration (Fig. 5A–C), which became more pronounced in aged mice (Fig. 1D–F). We did not detect dopaminergic neuron degeneration in 2-week-old *Sirt3*$^{-/-}$; *DJ-1*$^{-/-}$ double knockout mice, indicating that dopaminergic neuron loss in these mice at a later age was not due to developmental defects. Interestingly, we did not observe age-related dopaminergic neuron degeneration in *Sirt3*$^{-/-}$ or *DJ-1*$^{-/-}$ single knockout mice (Fig. 1), although these mice did exhibit compromised mitochondrial membrane potential (Fig. 5A–D) and increased mitochondrial oxidative stress (Fig. 4). These findings suggest that a threshold level of oxidative stress, higher than that in *Sirt3*$^{-/-}$ or *DJ-1*$^{-/-}$ single knockout mice, is required to trigger dopaminergic neuron degeneration. These observations also imply that Sirt3 and DJ-1 protect dopaminergic neurons from mitochondrial oxidative stress by different mechanisms. DJ-1 has been shown to attenuate the mitochondrial oxidative stress evoked by autonomous pacemaking by increasing the expression of mitochondrial uncoupling proteins (16). Here we found that Sirt3 protected dopaminergic neurons by deacetylating MnSOD K68 to increase its detoxicating activity (Fig. 6). Genetic removal of *Sirt3* in *DJ-1*$^{-/-}$ knockout mice further exacerbated oxidative stress in *Sirt3*$^{-/-}$; *DJ-1*$^{-/-}$ double knockout mice, leading to dopaminergic neuron degeneration after the threshold was passed.

These findings also may help explain the age-related late onset of PD. In human PD patients, dopaminergic neuron degeneration occurs only after the age-dependent accumulation of oxidative damages together with stress caused by mutations in PD genes (*DJ-1* or others) reach a critical threshold. Therefore, enhancing the protective function of Sirt3 may be used to keep oxidative stress below the threshold level to delay or prevent dopaminergic neuron degeneration in PD. The age-related degeneration of SNc dopaminergic neurons in *Sirt3*$^{-/-}$; *DJ-1*$^{-/-}$ double knockout mice implies that these mice might be used as a novel genetic model for studying PD.

Sirt3-mediated deacetylation of MnSOD K68 in dopaminergic neurons and the underlying biochemical mechanism

As a mitochondria-specific deacetylase, Sirt3 has been shown to regulate mitochondrial function and energy metabolism in hepatocytes, muscles and tumour cells (45–47). Here we focused on dopaminergic neurons because their relevance to PD. Sirt3 can deacetylate diverse substrates to affect distinct aspects of mitochondrial functions including ATP production (26,27), ETC activity (48,49), and amino acid metabolism (50). We and others have found that Sirt3 deacetylates and activates MnSOD to scavenge ROS in tumour cells (29–31,51). In this study, we demonstrate that Sirt3-mediated deacetylation of MnSOD K68 is particularly important for protecting dopaminergic neurons from their endogenous mitochondrial oxidative stress.

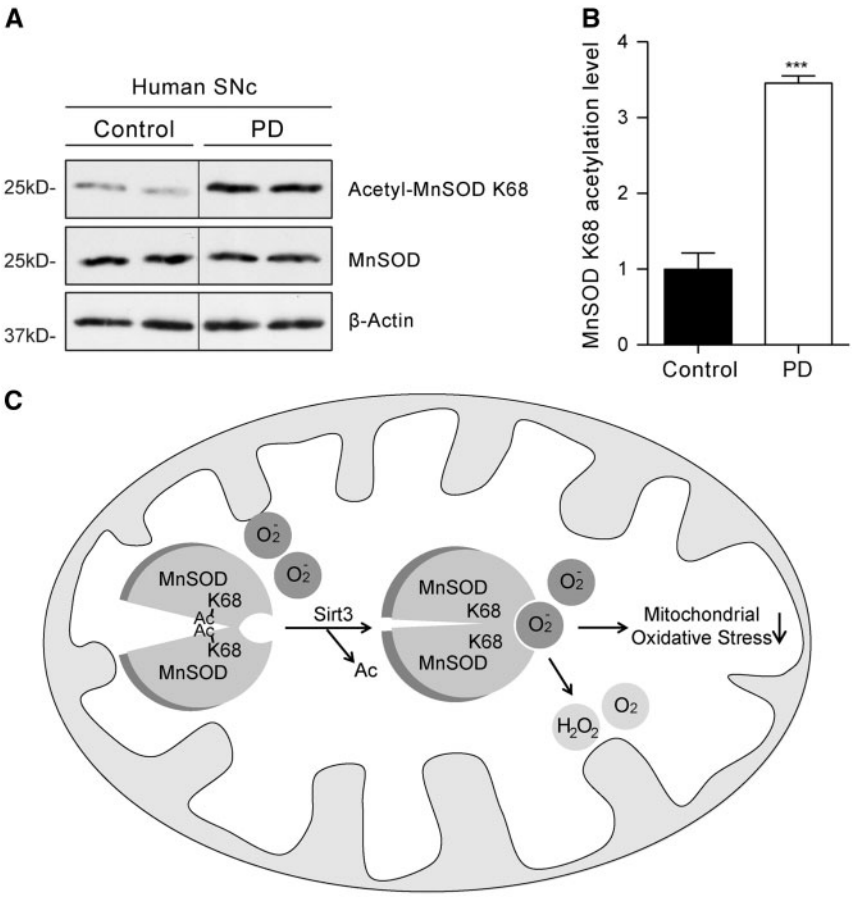

Figure 6. Increased acetylation of MnSOD K68 in PD patient substantia nigra and a working model. **(A)** Western blot analysis of MnSOD K68 acetylation levels in PD patient SNc and non-disease control human samples using the acetyl-MnSOD K68 specific antibody. **(B)** Quantification of Western blots showed significantly increased acetylation of MnSOD on lysine 68 in PD patient SNc compared with age-matched non-PD control human samples. **(C)** Working model for how Sirt3 protects ventral midbrain dopaminergic neurons from mitochondrial oxidative stress and degeneration by deacetylating MnSOD K68. Sirt3-mediated deacetylation of MnSOD on lysine 68 gives superoxide substrates better access to its enzymatic active site, leading to reduced mitochondrial oxidative stress in dopaminergic neurons.

Using *Sirt3*$^{-/-}$ knockout mouse SNc tissues, we observed reduced MnSOD activity and increased MnSOD K68 acetylation using our home-made acetyl-MnSOD K68 antibody (Figs 2 and 3). More importantly, we found that the expression of the deacetylation-mimetic MnSOD K68R mutant rescued phenotypes in *Sirt3*$^{-/-}$ knockout and *Sirt3*$^{-/-}$*; DJ-1*$^{-/-}$ double knockout mouse dopaminergic neurons, including the increased mitochondrial oxidative stress and decreased mitochondrial membrane potential (Figs 4 and 5). These observations demonstrate a critical role for Sirt3-mediated deacetylation of MnSOD K68 in protecting dopaminergic neurons from oxidative stress. The contributions of Sirt3 substrates other than MnSOD K68 remain to be explored.

How does the deacetylation of the evolutionarily conserved lysine 68 by Sirt3 affect MnSOD activity in dopaminergic neurons? In mitochondria, functional MnSOD binds one manganese ion per each of its four subunits (32). MnSOD scavenges the superoxide byproducts of OXPHOS and converts them to less toxic hydrogen peroxide and diatomic oxygen. Analysis of MnSOD structure suggested that lysine 68 is located close to the position of the helical hairpin that is critical for the funnel structure that leads ROS to the active site of MnSOD (33,34). Based on the structural importance of lysine 68, we hypothesize that the deacetylation of MnSOD K68 by Sirt3 may facilitate the access of substrates to MnSOD to enhance its detoxicating enzymatic activity (Fig. 6C). This facilitation could be due to deacetylation-induced conformational changes of MnSOD, or the positive charge of deacetylated lysine, which would attract more negatively charged superoxide to the active site of MnSOD (Fig. 6C).

Age-dependent accumulation of mitochondrial oxidative stress is widely viewed as a key contributor to the selective degeneration of dopaminergic neurons in both sporadic and familial forms of PD. Our findings revealed a critical role for Sirt3 in protecting dopaminergic neurons from mitochondrial oxidative stress by deacetylating MnSOD K68. The increased acetylation of MnSOD K68 we observed in PD patient SNc tissues suggests that age-related decline in Sirt3 protective function may contribute to dopaminergic neuron degeneration in PD. Therefore, enhancing the protective mechanism may represent a new therapeutic strategy for protecting dopaminergic neurons from degeneration.

Materials and Methods

Mouse models and human midbrain samples

The *Sirt3* knockout mice (*Sirt3*$^{-/-}$ Jackson Laboratory no. 012755) (25) and *DJ-1* knockout mouse model (*DJ-1*$^{-/-}$, Jackson Laboratory no. 006577) (52) were obtained from the Surmeier Laboratory. Genomic DNA extracted from tail samples was used

for PCR-based genotyping following the protocols from the Jackson Laboratory. Human midbrain tissue samples from PD patients and control individuals were obtained through collaboration with The Human Brain Resource Center. Samples from three PD patients (76 years old with postmortem interval (PMI) of 14 h; 85 years old with PMI of 19.3 h; 82 years old with PMI of 13.7 h) and three control individuals (75 years old with PMI of 15.4 h; 80 years old with PMI of 12 h; 80 years old with PMI of 18.75 h) were used.

DAB immunohistochemical and Nissl staining

Immunohistochemical staining was performed using the Vectastain ABC HRP Kit (Vector Labs). Before staining, sections were soaked in 0.3% hydrogen peroxide (H_2O_2) aqueous solution for 20 min. After washing with PBS, sections were transferred into a blocking solution containing 5% goat serum in PBS for 30 min, followed by incubation with a rabbit anti-TH antibody (Millipore/Chemicon AB152) at 4 °C overnight. Then after washing with PBS, tissue sections were incubated with biotinylated goat antirabbit IgG antibody (Vector Labs) for one hour at room temperature, followed by incubation with ABC peroxidase complex (Vector Labs) for 30 min. Tissue sections were then transferred into the DAB (3,3′-diaminobenzidine, Sigma) solution, gently shaken until desired stain intensity was developed, rinsed with PBS, and mounted onto Superfrost Plus microscope slides (Fisher Scientific) for imaging.

Nissl staining solution was freshly prepared by dissolving cresyl violet (Sigma) in an appropriate amount of distilled water to make the final concentration of 10 g/l. After overnight stirring, glacial acetic acid was added to the solution to a final concentration of 10 ml/l. Tissue sections cut with microtome were mounted onto Superfrost Plus microscope slides (Fisher Scientific) and air-dried for 24 h. Slides carrying tissue sections were dipped into Nissl solution for 1 min. Then slides were removed from the solution, briefly rinsed in distilled water, and washed sequentially in 50, 70 and 95% ethanol. Slides were finally destained in 100% ethanol until reaching the desired level of staining.

Western blotting

Tissue or cell samples were lysed in RIPA buffer (150 mM NaCl, 1% NP-40, 0.5% sodium deoxycholate, 0.1% SDS, 50 mM Tris, pH 7.5, 1mM EDTA, 5 mM DTT, 10 mM NaF and 1 mM Na_3VO_4, protease inhibitor cocktail tablet (Roche)) for Western blot analysis. Tissue samples were homogenized using a Polytron homogenizer (Kinematica). Protein concentrations were quantified using the BCA protein assay kit (Pierce). Each sample was denatured at 95 °C for 5 min before loading onto freshly prepared 10% SDS-PAGE gel for protein separation. Separated proteins on SDS-PAGE were transferred onto polyvinylidene fluoride membrane, and incubated with the indicated antibody. Primary antibodies were diluted in TBS containing 0.05% Tween-20 and 5% BSA. Primary antibodies used in this study include anti-acetyl-MnSOD K68 (1:200, rabbit monoclonal, Gius Laboratory/Abcam), anti-MnSOD (1:500, rabbit polyclonal, Millipore), and anti-β-actin (1:1000, rabbit polyclonal, Abcam). Horseradish peroxidase (HRP)-conjugated secondary antibodies (1:10 000; Jackson ImmunoResearch) and the Femto LUCENT plus HRP reagent kit (G-Biosciences) were used for exposure and quantification by densitometry.

Superoxide dismutase activity assay

Midbrain tissues or cells were homogenized in prechilled homogenization buffer containing 20mM HEPES, pH 7.2, containing 1mM EGTA, 210 mM mannitol and 70 mM sucrose. Lysates were centrifuged at 1500 × g for 5 min at 4 °C. Then supernatants were transferred into another tube for centrifuge at 10 000 × g for 15 min at 4 °C. The precipitated pellets contain mitochondrial MnSOD while the supernatants contain cytosolic SODs. Pellets were then resuspended in prechilled homogenization HEPES buffer and sonicated to release the mitochondrial contents. The Superoxide Dismutase Assay Kit (Cayman Chemical) was used to quantify the activity of each type of SOD following manufacturer's instructions. Briefly, samples were loaded onto a 96-well plate and mixed with reaction agents and incubated at room temperature for 30 min on a shaker. Absorbance was measured at the wavelength of 450 nm. Activities of SODs were calculated based on the standard curve.

Primary dopaminergic neuron and MN9D cell culture

Postnatal days 1–3 (P1–P3) mice were anesthetized and decapitated for brain harvesting. Mouse substantia nigra or striatal regions were carefully micro-dissected out based on anatomical hallmarks and minced in Hibernate A medium (Invitrogen). Papain dissociation medium containing 20 U/ml papain (Worthington Biochemical), 2 U/ml DNase I and 0.5 mM EDTA in Hibernate A medium was prepared before brain dissection. Papain dissociation medium was incubated at 37 °C until clear, then L-cysteine was added to 1 mM into dissociation medium to activate papain 10 min before use. All tissues were digested with the activated papain dissociation medium at 37 °C for 20 min, with occasional shaking. Digested tissues were then centrifuged at 200 × g for 3 min to precipitate. The supernatant was then replaced with fresh Hibernate A medium. Tissues were then triturated with fire-polished glass pipettes. Substantia nigral and striatal neurons were resuspended, mixed at a ratio of 3:1, and plated on 12 mm coverglasses precoated with 0.1% polyethylenimine (Sigma) at a density of 200 000 cells per coverslip. Coverslips were placed in a 24-well plate containing prewarmed growth medium containing Neurobasal A medium (Invitrogen) supplemented with B27 (Invitrogen), 0.5 mM glutamine, 50 μg/ml BDNF, 50 μg/ml CNTF and 25 μg/ml GDNF (PeproTech). After the initial plating, half of the medium was exchanged with fresh supplemented Neurobasal A growth medium every 3 days. Plates were incubated at 37 °C with 5% CO_2. MN9D mouse dopaminergic neuron cell line (35) was cultured in DMEM (Cellgro) supplemented with 10% fetal bovine serum at 37 °C with 5% CO_2. Cells were transfected with Lipofectamine 2000 (Life Technologies) following manufacturer's instructions. Cell death was detected by the *in situ* cell death detection TMR red TUNEL (Terminal Transferase dUTP Nick End Labelling) kit (Roche) 48 h after transfection.

Mitochondrial oxidative stress measurement

Primary mouse midbrain neurons cultured on glass coverslips for 3–4 days were infected with AAV expressing a roGFP with a mitochondria matrix targeting sequence driven by a TH-promoter (AAV-TH-mito-roGFP) (53). Two days after transduction, cultured neurons were transferred to an imaging chamber with inverted epifluorescence microscope (Olympus IX71) using a 40X/NA 1.35 oil-immersion objective (Olympus). Cultured neurons were perfused with artificial cerebrospinal

fluid (ACSF) containing 125 mM NaCl, 3 mM KCl, 1.25 mM NaH_2PO_4, 25 mM $NaHCO_3$, 1 mM $MgCl_2$, 2 mM $CaCl_2$ and 25 mM D-glucose, pH 7.4. Neurons were kept in ACSF for 10 min to allow fluid environment reaching equilibrium before imaging. All experiments were performed at 35–36 °C. Two excitation wavelengths (410 and 470 nm) were used with emission monitored at 535 nm. Region of interests were selected using imaging software SlideBook (Intelligent Imaging Innovations). Images were taken every 30 s using a cooled CCD camera (I-PentaMax, Princeton Instruments) and fluorescent intensities were measured ratiometrically. After initial measurements at basal level, neuron cultures were treated with 2 mM dithiothreitol (DTT) to get fully reduced, followed by 100 μM aldrithiol treatment to reach maximal oxidation. Fluorescent intensities were measured correspondingly to determine the range of roGFP signal. The relative mitochondrial oxidative levels were then calculated as $1 - [(F - F_{Ald})/(F_{DTT} - F_{Ald})]$, in which F, F_{DTT} and F_{Ald} represent measured intensities at basal, reduced and oxidized states, respectively.

Mitochondrial membrane potential measurement

Mitochondrial membrane potential was measured with the potential-dependent fluorescent dye TMRE (Molecular Probes). Cultured mouse SNc neurons expressing TH-mito-roGFP were incubated with 200 nM TMRE in phenol red-free Neuorobasal medium (Thermo Fisher Scientific) for 30 min. Neurons on coverslips were then transferred to a LSM 800 confocal microscope (Zeiss) for live imaging. Neurons with TH-mito-roGFP expression were considered as dopaminergic neurons and selected for recording. The excitation wavelength was set to 550 nm and with emission monitored at 570 nm. Baseline intensities of fluorescent signals were determined by treating neurons with 10 μM rotenone for 15 min.

Acknowledgements

We thank Dr Zhong Xie for his help with measuring mitochondrial oxidative stress in neurons, Dr Jyothisri Kondapalli for providing the AAV-mito-roGFP and Dr Yueming Zhu for the Sirt3 and MnSOD expression constructs.

Conflict of Interest statement. None declared.

Funding

This work was supported by National Institutes of Health (grant numbers AG043970 and R01NS094564) and grants from The Hartwell Foundation, the Chicago Biomedical Consortium and Whitehall Foundation to Y.C.M. Y.C.M. is Ann Marie and Francis Klocke M.D. Research Scholar supported by the Joseph and Bessie Feinberg Foundation. D.G. is supported by National Institutes of Health (grant numbers 2R01CA152601-A1, 1R01CA152799-01A1, 1R01CA168292-01A1, 1R01CA214025-01), the Chicago Biomedical Consortium, Zell Family Foundation, the Lynn Sage Foundation, the Avon Foundation and the Searle Funds at The Chicago Community Trust. D.J.S. is supported by National Institutes of Health (grant number NS047085) and JPB Foundation.

References

1. de Lau, L.M. and Breteler, M.M. (2006) Epidemiology of Parkinson's disease. *Lancet Neurol.*, **5**, 525–535.
2. de Rijk, M.C., Breteler, M.M., Graveland, G.A., Ott, A., Grobbee, D.E., van der Meche, F.G. and Hofman, A. (1995) Prevalence of Parkinson's disease in the elderly: the Rotterdam Study. *Neurology*, **45**, 2143–2146.
3. Riederer, P. and Wuketich, S. (1976) Time course of nigrostriatal degeneration in parkinson's disease. A detailed study of influential factors in human brain amine analysis. *J. Neural Transm.*, **38**, 277–301.
4. Hornykiewicz, O. (1966) Dopamine (3-hydroxytyramine) and brain function. *Pharmacol. Rev.*, **18**, 925–964.
5. Fahn, S. (1986) *Recent developments in Parkinson's disease*. Raven Press, New York, NY.
6. Moore, D.J., West, A.B., Dawson, V.L. and Dawson, T.M. (2005) Molecular pathophysiology of Parkinson's disease. *Annu. Rev. Neurosci.*, **28**, 57–87.
7. Sheng, Z.H. and Cai, Q. (2012) Mitochondrial transport in neurons: impact on synaptic homeostasis and neurodegeneration. *Nat. Rev. Neurosci.*, **13**, 77–93.
8. Mishra, P. and Chan, D.C. (2014) Mitochondrial dynamics and inheritance during cell division, development and disease. *Nat. Rev. Mol. Cell. Biol.*, **15**, 634–646.
9. Bender, A., Krishnan, K.J., Morris, C.M., Taylor, G.A., Reeve, A.K., Perry, R.H., Jaros, E., Hersheson, J.S., Betts, J., Klopstock, T. *et al.* (2006) High levels of mitochondrial DNA deletions in substantia nigra neurons in aging and Parkinson disease. *Nat. Genet.*, **38**, 515–517.
10. Kraytsberg, Y., Kudryavtseva, E., McKee, A.C., Geula, C., Kowall, N.W. and Khrapko, K. (2006) Mitochondrial DNA deletions are abundant and cause functional impairment in aged human substantia nigra neurons. *Nat. Genet.*, **38**, 518–520.
11. Swerdlow, R.H., Parks, J.K., Miller, S.W., Tuttle, J.B., Trimmer, P.A., Sheehan, J.P., Bennett, J.P., Jr., Davis, R.E. and Parker, W.D. Jr. (1996) Origin and functional consequences of the complex I defect in Parkinson's disease. *Ann. Neurol.*, **40**, 663–671.
12. Ryan, B.J., Hoek, S., Fon, E.A. and Wade-Martins, R. (2015) Mitochondrial dysfunction and mitophagy in Parkinson's: from familial to sporadic disease. *Trends Biochem. Sci.*, **40**, 200–210.
13. Hauser, D.N. and Hastings, T.G. (2013) Mitochondrial dysfunction and oxidative stress in Parkinson's disease and monogenic parkinsonism. *Neurobiol. Dis.*, **51**, 35–42.
14. Schapira, A.H. (2008) Mitochondria in the aetiology and pathogenesis of Parkinson's disease. *Lancet Neurol.*, **7**, 97–109.
15. Chan, C.S., Guzman, J.N., Ilijic, E., Mercer, J.N., Rick, C., Tkatch, T., Meredith, G.E. and Surmeier, D.J. (2007) 'Rejuvenation' protects neurons in mouse models of Parkinson's disease. *Nature*, **447**, 1081–1086.
16. Guzman, J.N., Sanchez-Padilla, J., Wokosin, D., Kondapalli, J., Ilijic, E., Schumacker, P.T. and Surmeier, D.J. (2010) Oxidant stress evoked by pacemaking in dopaminergic neurons is attenuated by DJ-1. *Nature*, **468**, 696–700.
17. Abou-Sleiman, P.M., Healy, D.G., Quinn, N., Lees, A.J. and Wood, N.W. (2003) The role of pathogenic DJ-1 mutations in Parkinson's disease. *Ann. Neurol.*, **54**, 283–286.
18. Bonifati, V., Rizzu, P., van Baren, M.J., Schaap, O., Breedveld, G.J., Krieger, E., Dekker, M.C., Squitieri, F., Ibanez, P., Joosse, M. *et al.* (2003) Mutations in the DJ-1 gene associated with autosomal recessive early-onset parkinsonism. *Science*, **299**, 256–259.
19. Kitada, T., Asakawa, S., Hattori, N., Matsumine, H., Yamamura, Y., Minoshima, S., Yokochi, M., Mizuno, Y. and

Shimizu, N. (1998) Mutations in the parkin gene cause autosomal recessive juvenile parkinsonism. *Nature*, **392**, 605–608.
20. Valente, E.M., Abou-Sleiman, P.M., Caputo, V., Muqit, M.M., Harvey, K., Gispert, S., Ali, Z., Del Turco, D., Bentivoglio, A.R., Healy, D.G. *et al.* (2004) Hereditary early-onset Parkinson's disease caused by mutations in PINK1. *Science*, **304**, 1158–1160.
21. Chang, H.C. and Guarente, L. (2013) SIRT1 and other sirtuins in metabolism. *Trends Endocrinol. Metab*, **25**, 138–145.
22. Michan, S. and Sinclair, D. (2007) Sirtuins in mammals: insights into their biological function. *Biochem. J.*, **404**, 1–13.
23. Yoshino, J. and Imai, S. (2011) Mitochondrial SIRT3: a new potential therapeutic target for metabolic syndrome. *Mol. Cell*, **44**, 170–171.
24. Bell, E.L. and Guarente, L. (2011) The SirT3 divining rod points to oxidative stress. *Mol. Cell*, **42**, 561–568.
25. Lombard, D.B., Alt, F.W., Cheng, H.L., Bunkenborg, J., Streeper, R.S., Mostoslavsky, R., Kim, J., Yancopoulos, G., Valenzuela, D., Murphy, A. *et al.* (2007) Mammalian Sir2 homolog SIRT3 regulates global mitochondrial lysine acetylation. *Mol. Cell Biol.*, **27**, 8807–8814.
26. Vassilopoulos, A., Pennington, J.D., Andresson, T., Rees, D.M., Bosley, A.D., Fearnley, I.M., Ham, A., Flynn, C.R., Hill, S., Rose, K.L. *et al.* (2014) SIRT3 deacetylates ATP synthase F1 complex proteins in response to nutrient- and exercise-induced stress. *Antioxid. Redox. Signal.*, **21**, 551–564.
27. Rahman, M., Nirala, N.K., Singh, A., Zhu, L.J., Taguchi, K., Bamba, T., Fukusaki, E., Shaw, L.M., Lambright, D.G., Acharya, J.K. *et al.* (2014) Drosophila Sirt2/mammalian SIRT3 deacetylates ATP synthase beta and regulates complex V activity. *J. Cell Biol.*, **206**, 289–305.
28. Spitz, D.R. and Oberley, L.W. (1989) An assay for superoxide dismutase activity in mammalian tissue homogenates. *Anal. Biochem.*, **179**, 8–18.
29. Chen, Y., Zhang, J., Lin, Y., Lei, Q., Guan, K.L., Zhao, S. and Xiong, Y. (2011) Tumour suppressor SIRT3 deacetylates and activates manganese superoxide dismutase to scavenge ROS. *EMBO Rep.*, **12**, 534–541.
30. Lone, M.U., Baghel, K.S., Kanchan, R.K., Shrivastava, R., Malik, S.A., Tewari, B.N., Tripathi, C., Negi, M.P., Garg, V.K., Sharma, M. *et al.* (2016) Physical interaction of estrogen receptor with MnSOD: implication in mitochondrial O2.- upregulation and mTORC2 potentiation in estrogen-responsive breast cancer cells. *Oncogene*, 10.1038/onc.2016.346.
31. Lu, J., Cheng, K., Zhang, B., Xu, H., Cao, Y., Guo, F., Feng, X. and Xia, Q. (2015) Novel mechanisms for superoxide-scavenging activity of human manganese superoxide dismutase determined by the K68 key acetylation site. *Free Radic. Biol. Med.*, **85**, 114–126.
32. Sato, S. and Nakazawa, K. (1978) Purification and properties of superoxide dismutase from Thermus thermophilus HB8. *J. Biochem.*, **83**, 1165–1171.
33. Borgstahl, G.E., Parge, H.E., Hickey, M.J., Beyer, W.F., Jr., Hallewell, R.A. and Tainer, J.A. (1992) The structure of human mitochondrial manganese superoxide dismutase reveals a novel tetrameric interface of two 4-helix bundles. *Cell*, **71**, 107–118.
34. Zhu, Y., Park, S.H., Ozden, O., Kim, H.S., Jiang, H., Vassilopoulos, A., Spitz, D.R. and Gius, D. (2012) Exploring the electrostatic repulsion model in the role of Sirt3 in directing MnSOD acetylation status and enzymatic activity. *Free Radic. Biol. Med.*, **53**, 828–833.
35. Choi, H.K., Won, L., Roback, J.D., Wainer, B.H. and Heller, A. (1992) Specific modulation of dopamine expression in neuronal hybrid cells by primary cells from different brain regions. *Proc. Natl. Acad. Sci. U. S. A.*, **89**, 8943–8947.
36. Abou-Sleiman, P.M., Muqit, M.M. and Wood, N.W. (2006) Expanding insights of mitochondrial dysfunction in Parkinson's disease. *Nat. Rev. Neurosci.*, **7**, 207–219.
37. Michel, P.P. and Hefti, F. (1990) Toxicity of 6-hydroxydopamine and dopamine for dopaminergic neurons in culture. *J. Neurosci. Res.*, **26**, 428–435.
38. Zecca, L., Zucca, F.A., Wilms, H. and Sulzer, D. (2003) Neuromelanin of the substantia nigra: a neuronal black hole with protective and toxic characteristics. *Trends Neurosci.*, **26**, 578–580.
39. Greenamyre, J.T. and Hastings, T.G. (2004) Biomedicine. Parkinson's–divergent causes, convergent mechanisms. *Science*, **304**, 1120–1122.
40. Liu, L., Peritore, C., Ginsberg, J., Kayhan, M. and Donmez, G. (2015) SIRT3 attenuates MPTP-induced nigrostriatal degeneration via enhancing mitochondrial antioxidant capacity. *Neurochem. Res.*, **40**, 600–608.
41. Zhang, X., Ren, X., Zhang, Q., Li, Z., Ma, S., Bao, J., Li, Z., Bai, X., Zheng, L., Zhang, Z. *et al.* (2016) PGC-1alpha/ERRalpha-Sirt3 pathway regulates DAergic neuronal death by directly deacetylating SOD2 and ATP synthase beta. *Antioxid. Redox. Signal.*, **24**, 312–328.
42. Forno, L.S., DeLanney, L.E., Irwin, I. and Langston, J.W. (1993) Similarities and differences between MPTP-induced parkinsonsim and Parkinson's disease. Neuropathologic considerations. *Adv. Neurol.*, **60**, 600–608.
43. Langston, J.W. and Irwin, I. (1986) MPTP: current concepts and controversies. *Clin. Neuropharmacol.*, **9**, 485–507.
44. Przedborski, S. and Jackson-Lewis, V. (1998) Mechanisms of MPTP toxicity. *Mov. Disord.*, **13(Suppl 1)**, 35–38.
45. Jing, E., Emanuelli, B., Hirschey, M.D., Boucher, J., Lee, K.Y., Lombard, D., Verdin, E.M. and Kahn, C.R. (2011) Sirtuin-3 (Sirt3) regulates skeletal muscle metabolism and insulin signaling via altered mitochondrial oxidation and reactive oxygen species production. *Proc. Natl. Acad. Sci. U. S. A.*, **108**, 14608–14613.
46. Hirschey, M.D., Shimazu, T., Jing, E., Grueter, C.A., Collins, A.M., Aouizerat, B., Stancakova, A., Goetzman, E., Lam, M.M., Schwer, B. *et al.* (2011) SIRT3 deficiency and mitochondrial protein hyperacetylation accelerate the development of the metabolic syndrome. *Mol. Cell*, **44**, 177–190.
47. Kim, H.S., Patel, K., Muldoon-Jacobs, K., Bisht, K.S., Aykin-Burns, N., Pennington, J.D., van der Meer, R., Nguyen, P., Savage, J., Owens, K.M. *et al.* (2010) SIRT3 is a mitochondria-localized tumor suppressor required for maintenance of mitochondrial integrity and metabolism during stress. *Cancer Cell*, **17**, 41–52.
48. Finley, L.W., Haas, W., Desquiret-Dumas, V., Wallace, D.C., Procaccio, V., Gygi, S.P. and Haigis, M.C. (2011) Succinate dehydrogenase is a direct target of sirtuin 3 deacetylase activity. *PLoS One*, **6**, e23295.
49. Ahn, B.H., Kim, H.S., Song, S., Lee, I.H., Liu, J., Vassilopoulos, A., Deng, C.X. and Finkel, T. (2008) A role for the mitochondrial deacetylase Sirt3 in regulating energy homeostasis. *Proc. Natl. Acad. Sci. U. S. A.*, **105**, 14447–14452.
50. Hallows, W.C., Yu, W., Smith, B.C., Devries, M.K., Ellinger, J.J., Someya, S., Shortreed, M.R., Prolla, T., Markley, J.L., Smith, L.M. *et al.* (2011) Sirt3 promotes the urea cycle and fatty acid oxidation during dietary restriction. *Mol. Cell*, **41**, 139–149.
51. Tao, R., Coleman, M.C., Pennington, J.D., Ozden, O., Park, S.H., Jiang, H., Kim, H.S., Flynn, C.R., Hill, S., Hayes McDonald, W. *et al.* (2010) Sirt3-mediated deacetylation of evolutionarily conserved lysine 122 regulates MnSOD activity in response to stress. *Mol. Cell*, **40**, 893–904.

52. Andres-Mateos, E., Perier, C., Zhang, L., Blanchard-Fillion, B., Greco, T.M., Thomas, B., Ko, H.S., Sasaki, M., Ischiropoulos, H., Przedborski, S. *et al.* (2007) DJ-1 gene deletion reveals that DJ-1 is an atypical peroxiredoxin-like peroxidase. *Proc. Natl. Acad. Sci. U. S. A.*, **104**, 14807–14812.

53. Dryanovski, D.I., Guzman, J.N., Xie, Z., Galteri, D.J., Volpicelli-Daley, L.A., Lee, V.M., Miller, R.J., Schumacker, P.T. and Surmeier, D.J. (2013) Calcium entry and alpha-synuclein inclusions elevate dendritic mitochondrial oxidant stress in dopaminergic neurons. *J. Neurosci.*, **33**, 10154–10164.